# Effect of interchain interactions on the absorption and emission of poly(3-hexylthiophene)

Peter J. Brown,* D. Steve Thomas, Anna Köhler, Joanne S. Wilson, Ji-Seon Kim,
Catherine M. Ramsdale, Henning Sirringhaus,† and Richard H. Friend
*University of Cambridge, Cavendish Laboratory, Madingley Road, Cambridge, Cambridgeshire, United Kingdom CB3 0HE*
(Received 27 February 2002; published 28 February 2003)

The absorption spectrum of polythiophene and its derivative poly(3-hexylthiophene) (P3HT) is usually described in terms of an intrachain exciton coupled to a single phonon mode. We show that this model is too simplistic for highly ordered, regioregular P3HT and that, analogous to the case of charged polarons in this material, interchain interactions must be taken into account to correctly describe the absorption spectrum. We show that the lowest energy feature in the $\pi$-$\pi^*$ region of the absorption spectrum is associated with an interchain absorption, the intensity of which is correlated with the degree of order in the polymer. Correspondingly, we show that the emission from P3HT also exhibits contributions from both interchain and intrachain states, in a manner similar to that recently shown for poly(phenylenevinylene). Having reinterpreted the physical origin of the features in the absorption and emission spectra of P3HT, we then model these spectra and show how they evolve as the degree of order in the polymer is changed by varying several physical parameters including temperature and regioregularity of the polymer.

DOI: 10.1103/PhysRevB.67.064203 PACS number(s): 36.20.Kd, 33.20.Kf, 33.20.Tp, 85.30.Tv

## I. INTRODUCTION

The synthesis of highly regio-regular $2-5'$ head-to-tail coupled poly(3-hexylthiophene) (P3HT; see Fig. 1 for the structure)[1–3] has advanced the technology of polymeric field-effect transistors (FETs) to the extent that field-effect mobilities now reach 0.1 $cm^2/V\,s$ (Refs. 4 and 5), approximating that of $\alpha$-Si. This is three to four orders of magnitude higher than the original polythiophene (PT) FET,[6] and has been attributed to the high degree of intra and interchain order in the films. X-ray analysis has interpreted the structure of the polymer films as being composed of microcrystalline domains embedded in an amorphous matrix; inside these microcrystalline regions the polymers $\pi$ stack in one direction, and form lamella of interlocking side chains in the other.[2,7]

These $\pi$-stacked polymer chains provide an environment for increased interchain interactions and optical spectroscopy has shown that polarons in P3HT can no longer be considered as quasi-one-dimensional entities isolated on single chains; rather they are quasi-two-dimensional species influenced by the presence of neighboring polymer chains.[8–10] The explanation of the bulk absorption spectrum, however, still employs an intrachain excitonic model of isolated chains such that the fine structure in the $\pi$-$\pi^*$ absorption band is attributed to an optically excited state Franck-Condon coupled to a phonon mode.[11–13] A more detailed analysis of this simple model reveals that this cannot be the complete picture.

First, the nominal 0-0 feature appears to have a different temperature dependence from that of the other features.[14–18] Indeed, some authors have explicitly commented on this behavior, notably Salaneck *et al.*[14] and Inganäs *et al.*[15] They showed that when a P3HT film is heated from room temperature towards the glass transition temperature the polymer undergoes a rod to coil transition, generally resulting in a blue-shift and broadening of the main $\pi$-$\pi^*$ absorption band. However, these authors also noted that the least energetic absorption feature did not follow this trend in that it was not completely bleached and also remained at a constant energy. The same changes in the absorption spectra were noted when the coil to rod transition was induced by varying the amount of ''poor'' solvent in a well dissolved solution of poly(3-alkylthiophene).[15,18,19]

Second, the spacing of the fine structure features in the $\pi$-$\pi^*$ region of the solid-state, thin-film absorption spectrum of regioregular P3HT is not regular. Previously reported charge modulation spectroscopy (CMS) data[10] (which can achieve greater resolution of the fine structure than bulk absorption spectroscopy) puts the separation between the nominal 0-0 and 0-1 features at 0.17 eV, but at only 0.13 eV between the 0-1 and 0-2 features. This may be passed off as just coupling to two or more phonon modes, however other authors have noted that this spacing in the solid-state absorption and emission spectra of PT with reduced interchain interactions are regular, and therefore that the spectra of PT should be modeled by only one phonon mode coupled to the $\pi$-$\pi^*$ transition.[11,20–24] It is important to note that only one P3HT chain is present in the unit cell and so there are no features in the absorption spectrum that are attributable to Davydov splitting.

Further, as will be shown in this paper, if the absorption spectrum of P3HT is subjected to a Franck-Condon analysis, assuming the first feature is the 0-0 transition, then the relaxation energy of the $S_0 \rightarrow S_1$ transition is found to be similar to, and sometimes greater than, those calculated for an isolated stilbene[25] (0.27 eV) or bithiophene[26,27] molecule (0.25 eV). This would appear to contradict quantum chemical calculations and fits to experimental data which suggest that increasing the conjugation length[25] and the magnitude of interchain interactions[28] should significantly reduce the relaxation energy.

In the light of the modifications required when modeling polarons in an environment experiencing strong interchain interactions, it is reasonable to ask whether similar modifications are required to fully characterize excitons in P3HT. We submit that the observations outlined above are evidence

 

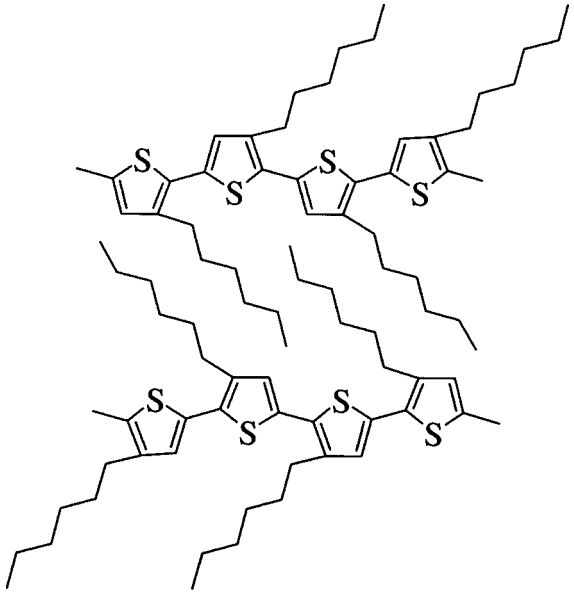

FIG. 1. Structure of regioregular head-to-tail coupled poly(3-hexylthiophene).

for the invalidity of the isolated chain, one-dimensional exciton model. These themes will be expanded upon in this paper, eventually demonstrating that the first feature in the $\pi$-$\pi^*$ absorption spectrum cannot be the 0-0 transition of an intrachain exciton. Indeed, the conclusion of this paper is that it is most likely due to an optical transition between states of an interchain nature and that the second feature in the main absorption band is the true origin of the $\pi$-$\pi^*$ intrachain absorption in P3HT.

Recently Ho *et al.*[29] showed that emission from an interchain exciton state was present in the photoluminescence (PL) spectrum of precursor route poly(phenylenevinylene). Complementary to this work, we shall demonstrate that this emission feature is also present in the PL spectrum of P3HT. Further, we shall show that the energies of the interchain 0-0 absorption and emission features are largely independent of intrinsic or extrinsic influence, whereas the corresponding features of the intrachain exciton are greatly dependent on the degree of intrachain order of the polymer chains.

Finally, by using this model to fit to charge modulation spectra of P3HT, a detailed analysis of how various physical parameters depend on small variations in the local order of the polymer chains will be discussed. Additionally, an improved analysis of the position and intensities of the charge-induced, subgap polaronic optical transitions will be obtained. This may allow a comparison to theoretical models of the charged species in P3HT.[30]

## II. EXPERIMENT

96% regioregular head-to-tail coupled P3HT (hereafter rrP3HT) was obtained from Aldrich Chemical Company and was synthesized via the Rieke route.[2] Regiorandom P3HT (hereafter rraP3HT) was obtained from the group of Prof. René Janssen at the Technical University of Eindhoven, the Netherlands. The polymer was obtained from the most soluble hexane fraction of 81% regioregular P3HT (prepared via the McCullough route[1]) undergoing purification via the Soxhlet process.

Films of these polymers were prepared by spin coating at a speed of 1500 rpm for one minute from a solution of chloroform at a concentration of 2–10 mg/ml depending on how thick a film was required (~30–80 nm). The films were annealed at 100 °C in a vacuum of $2\times10^{-6}$ mbar for 12 h to drive off any residual solvent and to promote a further self-ordering of the films. The substrates required for each experimental technique were rendered hydrophobic by methylating the surface, induced by exposure to hexamethyldisilazane (HMDS) at 175 °C for three hours.

*UV-vis absorption spectroscopy*. Absorption spectra were obtained using a Hewlett Packard 8453 uv-vis spectrometer. The samples were spin-coated spectrosil substrates.

*Raman spectroscopy*. Raman spectra were obtained using a Renishaw 2000 Raman Microscope. Spin-coated spectrosil samples were illuminated in a 180° backscattering geometry by the 633-nm line of a He-Ne laser; spectra accumulation times were 5–10 s. Note that low laser power (<1 mW) was required to avoid the fluorescence background and to reduce possible photo-oxidation.

*Spectroscopic ellipsometry*. An M-2000 ellipsometer from J. A. Woollam Co. Ltd. was used to obtain the refractive index of the polymers as a function of photon energy. Samples were either spin-coated spectrosil or $Si/SiO_2$ FET substrates.

*Photoluminescence (PL) spectroscopy*. PL spectra were obtained by irradiating spin-coated spectrosil samples using an Ar-ion laser. The emitted light was collected by an optical fibre coupled to an ORIEL Instaspec IV which measured the energy density spectrum in units of $[\mu W\,cm^{-2}\,nm^{-1}]$. The samples were placed in a continuous flow He cryostat from Oxford Instruments; the temperature of the samples was monitored using a Si diode sited nearby in good thermal contact.

*Charge modulation spectroscopy*. This experimental technique is described in detail elsewhere,[31–33] as is the analysis of the features expected in the spectra of P3HT.[10] Briefly, an ac gate bias modulates the amount of charge in the accumulation layer of a metal-insulator-semiconductor (MIS) diode; this results in a modulation of the subgap, charge-induced polaronic optical absorption features that can then be detected using lock-in techniques. The devices required for this experiment are identical in design to those described by this group previously.[10] CMS is useful for studying the detail in the absorption spectrum of a polymer as it yields greater resolution of the fine structure than normal UV-vis spectroscopy.

## III. RESULTS AND DISCUSSION

### A. Absorption of poly(3-hexylthiophene)

The UV-vis absorption spectra in the region of the $\pi$-$\pi^*$ absorption of regioregular and regiorandom P3HT are shown in Fig. 2(a); complementary to this, refractive index spectra of these polymers obtained by ellipsometry are shown in Fig. 2(b). The differences in the absorption spectra are marked:

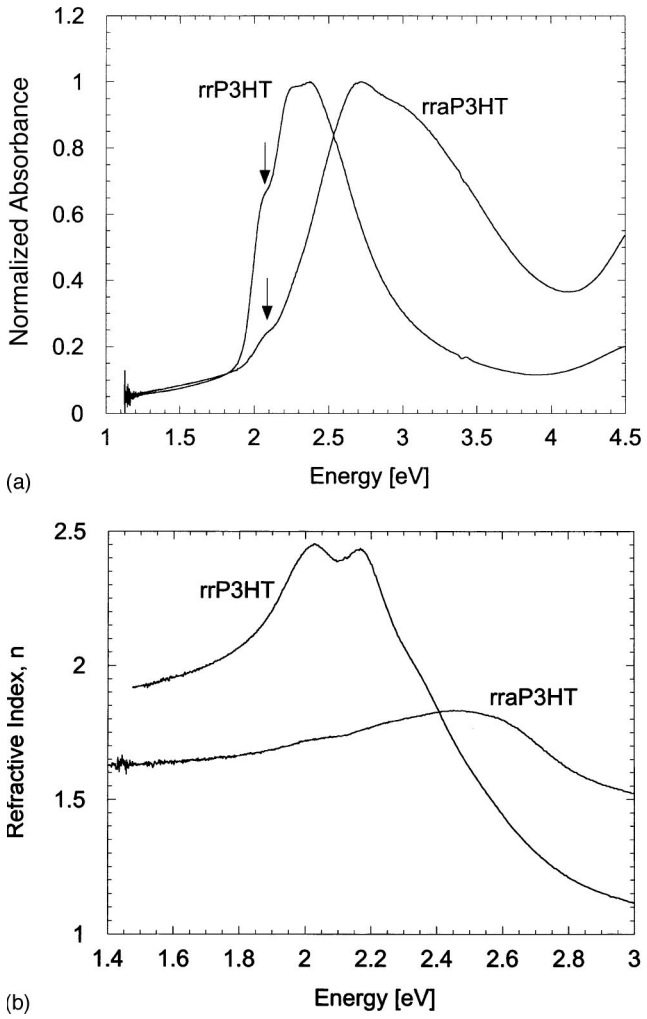


FIG. 2. (a) UV-vis absorption spectra of rr and rraP3HT, normalized to the maxima of the spectra. (b) Refractive index spectra of rr and rraP3HT, obtained using spectroscopic ellipsometry.

the absorption of rrP3HT is well structured with resolved features at ~2.09 (shoulder), 2.27, and ~2.37 eV, whereas rraP3HT is broader and less well resolved with a low-intensity shoulder at ~2.09 eV, a maximum at 2.72 eV, and a further shoulder at ~3.0 eV. Broadly speaking, it appears as if the rraP3HT spectrum is blueshifted with respect to the rrP3HT absorption, and this is usually attributed to a decrease in the effective conjugation lengths of the chain segments in the amorphous rraP3HT, localizing the wave function of the exciton to a greater extent and therefore increasing its energy. The less well-resolved fine structure in the rraP3HT spectrum can be attributed to an inhomogeneous broadening of the electronic $\pi$-$\pi^*$ transition caused by a relatively wider distribution of conjugation lengths at a lower mean length.

The interesting point about these spectra is that the feature at ~2.09 eV, indicated by an arrow in Fig. 2(a), appears to behave independently of the other features. Although it is less intense in the rraP3HT spectrum, with respect to the higher energy features, it does not appear to blueshift at all. This is similar to the behavior reported previously in the temperature dependence of solid-state spectra and the solvent

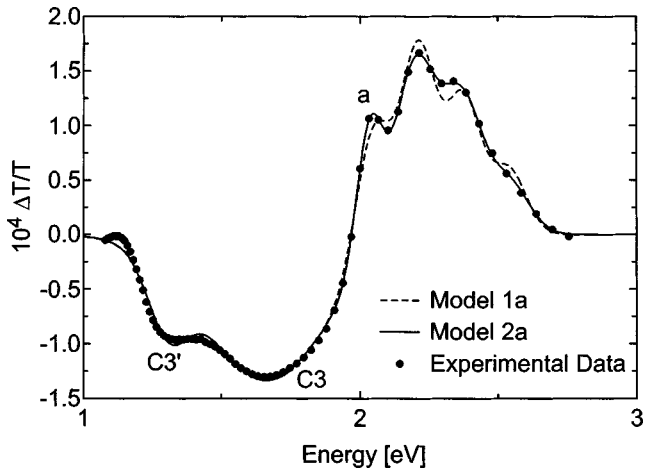


FIG. 3. CMS spectrum of rrP3HT in the visible range taken with an applied bias of $0\ \mathrm{V} \pm 1\ \mathrm{V}$ a.c. at a modulation frequency of 37 Hz at room temperature. The dashed and solid lines are fits to the data using models $1a$ and $2a$, respectively, as described in the text. Only every second data point is shown for clarity.

dependence of solution spectra.[14–18] This is a clear indication that the feature has a different physical origin than the other absorption features, indeed it also suggests that the origin is common to both polymers with only the intensity of the feature dependent on regioregularity and thus local order.

The fine structure in the absorption and emission spectra of conjugated molecules is described by Frank-Condon coupling. Frank-Condon coupled vibronic features are discussed in detail elsewhere,[34] but, in summary, the relative intensities of the features coupled by a single phonon are described by

$$\frac{I_{0\to n}}{I_0} = \frac{S^n e^{-s}}{n!}, \tag{1}$$

where $I_0$ is the total intensity of the individual transitions. $I_{0\to n}$ (shorthand for the transition from the 0 vibronic level in the $S_0$ electronic state to the $n$th vibronic level in $S_1$), is defined by

$$I_0 = \sum_{n=0}^{\infty} I_{0\to n}. \tag{2}$$

$S$ is the Huang Rhys parameter and is defined by

$$S = \frac{k(\Delta Q)^2}{2\hbar\omega_p} \tag{3}$$

where $k$ is the spring constant (assuming a two masses on a spring model for phonons), $\Delta Q$ is the change of the configuration coordinate from $S_0$ to $S_1$ and $\omega_p$ is the angular frequency of the phonon mode of energy $E_p$.

A typical CMS spectrum of rrP3HT is shown in Fig. 3. The features characterized by $\Delta T/T < 0$ at energies lower than 1.97 eV, labeled as $C3'$ and $C3$, are charge-induced polaronic absorption features, discussed in detail elsewhere.[10,30] Features characterized by $\Delta T/T > 0$ are the fine structure of the $\pi$-$\pi^*$ absorption described above, bleached by the presence of a polaron on the polymer chain.

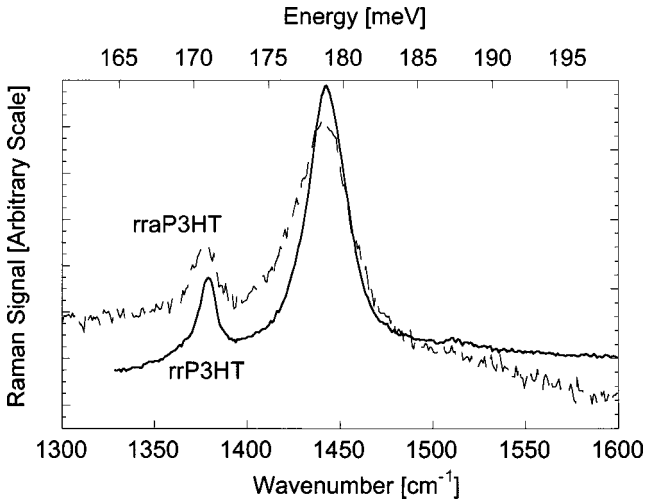


FIG. 4. Raman spectra of rr and rraP3HT.

The features are at 2.04 (labeled *a*), 2.21, and 2.34 eV, these are redshifted and far better resolved compared with the bulk absorption features as the field-induced charges occupy the lowest available energy states which correspond to the most ordered regions of the polymer in the microcrystalline domains. It is worth emphasizing again that there are no Davydov components in the absorption spectrum of P3HT as there is only one chain per unit cell.

Assuming only one phonon mode is coupled to the $\pi$-$\pi^*$ transition in rrP3HT (this shall be discussed in detail later in this section) and that the 0-0 transition is the least energetic absorption feature, labeled *a* in Fig. 4, this spectrum may be described as the sum of

(1) one Gaussian corresponding to $C3'$ [three parameters: height, position, and full width at half maximum (FWHM)],

(2) one Gaussian corresponding to $C3$ (three parameters), and

(3) a series of four Franck-Condon coupled Gaussians with the 0-0 transition corresponding to the feature at 2.04 eV (five parameters: total intensity $I_0$, energy of 0-0 transition $E_0$, Huang-Rhys parameter $S$, phonon energy $E_p$, and the FWHM of features).

This model shall be referred to as model 1*a* from here on. Gaussians were chosen to model the features as it is widely reported that strong electron-phonon coupling in conjugated polymers and other effects, such as inhomogeneous broadening, result in a Gaussian lineshape for transitions.[34] To check this, the imaginary dielectric constant spectrum of the bulk polymer, obtained from spectroscopic ellipsometry, was examined using both Lorentzians and Gaussians. While it was not possible to perform a full Franck-Condon analysis (the theory is defined for intensities only), a line-shape analysis revealed that Lorentzians yielded a very poor fit, consistent with the reports outlined above that optical features in the spectra of conjugated polymers have a Gaussian line shape. Nevertheless, Lorentzian line shapes were also used to model the features in the CMS spectra and, although the quality of fit was poorer, it is important to note that the conclusions discussed below were unchanged. Further, to obtain a Lorentzian broadened to $\sim$0.1 eV (the approximate width of the narrowest features in the spectrum) a lifetime of $7 \times 10^{-15}$ s is required, four to five orders of magnitude faster than the lifetime of excitons in similar conjugated materials.[19,24]

TABLE I. Best fit of the free parameters after modeling the CMS spectrum of rrP3HT taken at 0 V$\pm$1 V a.c., and 37 Hz, room temperature. The peak labeled "*a*" is the least energetic feature in the fine structure of the bleaching signal, as shown in Fig. 3. The uncertainty in the values are obtained from the standard deviation of the parameters after fitting. Also listed is the relaxation energy, $E_{\mathrm{rel}}=SE_p$, extracted from each model.

| Parameters | Model 1*a* | Model 2*a* |
|---|---|---|
| Height $C3'$ ($\times 10^4$) | $-0.600\pm0.03$ | $-0.56\pm0.02$ |
| Position $C3'$ (eV) | $1.303\pm0.003$ | $1.302\pm0.002$ |
| FWHM $C3'$ (eV) | $0.168\pm0.010$ | $0.154\pm0.007$ |
| Height $C3$ ($\times 10^4$) | $-1.334\pm0.014$ | $-1.3189\pm0.0098$ |
| Position $C3$ (eV) | $1.663\pm0.004$ | $1.657\pm0.003$ |
| FWHM $C3$ (eV) | $0.54\pm0.02$ | $0.555\pm0.0011$ |
| Height $a$ ($\times 10^4$) | | $1.30\pm0.03$ |
| Position $a$ (eV) | | $2.034\pm0.002$ |
| FWHM $a$ (eV) | | $0.116\pm0.004$ |
| $I_0$ ($\times 10^4$) | $5.156\pm0.098$ | $3.48\pm0.08$ |
| $E_0$ (eV) | $2.047\pm0.002$ | $2.199\pm0.003$ |
| $S$ | $1.41\pm0.02$ | $0.75\pm0.02$ |
| $E_p$ (eV) | $0.164\pm0.002$ | $0.170\pm0.002$ |
| FWHM (eV) | $0.148\pm0.003$ | $0.171\pm0.005$ |
| $E_{\mathrm{rel}}$ (eV) | $0.231\pm0.004$ | $0.128\pm0.004$ |

The best fit of the experimental data, obtained by allowing all the parameters to fit freely, is shown in Fig. 3, with the values of the parameters listed in Table I. It can be seen that the fit is not ideal as the structure in the bleaching signal is exaggerated and many of the peak positions poorly match the experimental features. An important parameter that can allow further examination of the model is the relaxation energy

$$E_{\mathrm{rel}}=SE_p. \tag{4}$$

$E_{\mathrm{rel}}$ is the average amount of energy by which the molecule relaxes to the lowest vibronic level of the upper electronic state upon absorption. From the values of $S$ and $E_p$ derived from model 1*a*, it can be seen that $E_{\mathrm{rel}}$ is 0.23 eV.

Cornil *et al.* performed extensive calculations on phenyl-capped poly(phenylenevinylene) (PPV) oligomers, and were able to extract the relaxation energy for several systems. The results can be summarized as follows: as the length of the oligomer chain increases $E_{\mathrm{rel}}$ decreases, for PPV2 (stilbene) $E_{\mathrm{rel}}=0.27$ eV, and for PPV5 $E_{\mathrm{rel}}=0.17$ eV; this was extrapolated to 0.14 eV for the isolated polymer.[25,35] In a polymer context this implies that $E_{\mathrm{rel}}$ decreases as the degree of intrachain order increases (that is, the effective conjugation length increases).

Also, for a system of two cofacial, interacting stilbene molecules $E_{\mathrm{rel}}$ decreases linearly from $\sim$0.245 to $\sim$0.195 eV as the interchain distance is reduced from 7.0 to 3.5 Å; the corresponding distance in P3AT has been shown to be $\sim$3.8 Å (Ref. 7). In a polymer context this implies that as the degree of interchain order increases, $E_{\mathrm{rel}}$ decreases.[28,36]

Calculations on isolated chains of thiophene oligomers[26,27] (*nT*, where *n* is the number of thiophene rings) have yielded relaxation energies of 0.25 eV for $2T$, 0.15 eV for $3T$, and 0.16 eV for $4T$. These values are of a similar order to the calculations on PPV oligomers, albeit slightly lower, but still show that $E_{\mathrm{rel}}$ decreases with increased conjugation length.

X-ray analysis, the high-field-effect mobility, and the identification of quasi-two-dimensional polaronic charge carriers in rrP3HT all suggest that rrP3HT is a polymer that exhibits high interchain and intrachain order, and this is certainly the case in the micro-crystalline regions probed by CMS. This suggests that the relaxation energy of rrP3HT should be toward the lower range of that calculated by Cornil *et al.*; however the large value of 0.23 eV extracted from model $1a$ is inconsistent with this.

As the feature at 2.04 eV (labeled *a* in Fig. 3) appears to be of a different physical origin from the other fine structure features in the $\pi$-$\pi^*$ absorption band, a better model to fit the CMS spectrum of rrP3HT may be to consider this not as the 0-0 transition, but as an independent Gaussian feature; the 0-0 origin may therefore be considered to be the feature at 2.21 eV. A free fit of these parameters, hereafter referred to as model $2a$, is also shown in Fig. 3, with the parameters listed in Table I. As Fig. 3 shows, this fit is closer to the experimental data; however, in isolation, this is not good evidence of a better model. What is significant is that the value of $E_{\mathrm{rel}}$ obtained from model $2a$ is $0.128 \pm 0.004$ eV and this is in far better agreement with the values calculated by Cornil *et al.* for a polymer exhibiting a high degree of intrachain and interchain order.

These models both rely on one crucial assumption, namely that only one phonon mode is coupled to the $\pi$-$\pi^*$ absorption of rrP3HT. Fourier transform infrared (FTIR) spectra[10] exhibit three features around the energy of $E_p$ derived from the models above, namely one weak feature at 0.171 eV and two stronger ones at 0.179 and 0.187 eV. The Raman spectrum of rrP3HT at similar energies is shown in Fig. 4. Two features are clearly observed, at 0.171 and 0.179 eV, with an intensity ratio of 1:8.5 (obtained by subtracting the background and fitting to Lorentzian curves). A close analysis of this spectrum reveals a very weak feature at 0.187 eV that is easily visible in the FTIR spectrum; in both spectra the feature at 0.179 eV is the strongest. This Raman spectrum is very similar to those published elsewhere[18,37,38] and the features can be assigned to the ring C-C stretch (0.171 eV), the symmetric C═C stretch (0.179 eV), and the antisymmetric C═C stretch (0.187 eV).

The total separation of these features is of the order of 15 meV whereas both models $1a$ and $2a$ show that the FWHM of the fine structure features is of the order of 150 meV, ten times greater. As a result, regardless of the relative weightings of these modes coupled to the $\pi$-$\pi^*$ absorption, they can all be modeled as a single mode. Other authors also reached a similar conclusion by studying the regularly spaced features in the absorption and emission spectra of PT and its derivatives[11,20,22–24] as well as the Raman spectrum.[21]

This is an important conclusion as it means that the relative merits of the two models of the CMS spectra can be discussed without having to incorporate further phonon modes into the Franck-Condon progressions. Indeed, this conclusion also allows the basis of model $1a$ to be called into question, as this model cannot explain the irregular spacing of the first three fine-structure features.

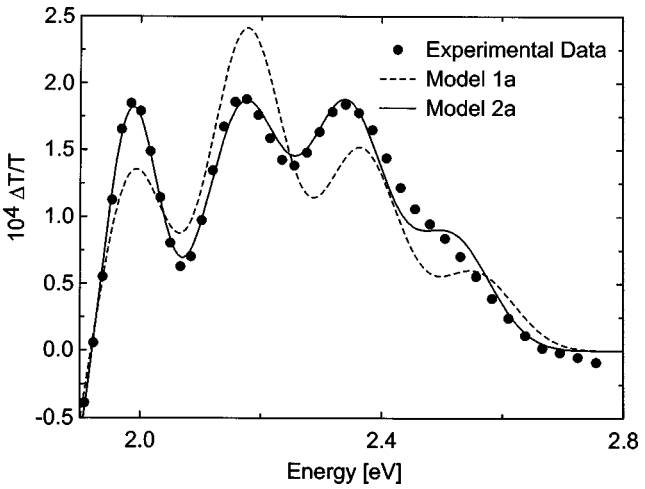


FIG. 5. Detail of the bleaching signal of the separated CMS spectrum of rrP3HT at 110 K after subtraction of the electroabsorption signal. Taken with an applied bias of $-2\,\mathrm{V} \pm 1\,\mathrm{V}$ a.c. at a modulation frequency of 37 Hz. The dashed and solid lines are fits to the data using models $1a$ and $2a$, respectively, as described in the text.

The value of $E_p$ derived from model $2a$ is lower by 0.01 eV than the value of 0.179 eV determined from the strongest feature in the Raman and FTIR spectra. This seems to reflect a softening of the phonon modes in the highly ordered microcrystalline regions with respect to the bulk amorphous polymer modes probed by Raman spectroscopy and FTIR. Put differently, this suggests a dispersion of the phonon mode energies with effective conjugation length, with the modes softening as intrachain order increases. Such a phenomenon has been observed in many conjugated polymers such as PT,[39,40] PPV (although, in this case, the effect is not large due to the specific intramolecular coupling),[41,42] polyacetylene, and polypyrrole[43,44] and hence this reduced value of $E_p$ is in good agreement with previous studies. As will be shown in Sec. III D, this effect can also be observed in the dc bias-dependent CMS spectrum of P3HT.

The temperature dependence of the CMS spectrum of rrP3HT is also interesting as temperature directly affects the degree of order in the film. This is because at low temperatures torsional rotations of the thiophene rings will be reduced in number, increasing the overlap of the wave functions of neighboring chains and hence the magnitude of the interchain interactions. It is difficult to fit the CMS spectrum at low temperature as an electroabsorption signal must be subtracted;[10] however where this is possible analysis of the pure charge-induced signal becomes easier. Figure 5 shows the separated bleaching signal of a spectrum taken at 110 K with two fits corresponding to models $1a$ and $2a$ (parameters of the fits are listed in Table II). The fit of model $1a$ is poor, indeed it cannot predict the relative heights and positions of the fine structure features at all. Model $2a$, however,

TABLE II. Best-fit values of the free parameters used to model the charge-induced features in the CMS spectrum of rrP3HT taken at 110 K with an applied bias of $-2\,\mathrm{V}\pm1\,\mathrm{V}$ a.c. at a frequency of 37 Hz, shown in Fig. 5.

| Parameters | Model 1*a* | Model 2*a* |
|---|---|---|
| Height $C3'$ ($\times10^4$) | $-0.5\pm0.1$ | $-0.69\pm0.04$ |
| Position $C3'$ (eV) | $1.316\pm0.008$ | $1.326\pm0.004$ |
| FWHM $C3'$ (eV) | $0.12\pm0.03$ | $0.165\pm0.010$ |
| Height $C3$ ($\times10^4$) | $-1.92\pm0.06$ | $-1.92\pm0.02$ |
| Position $C3$ (eV) | $1.78\pm0.04$ | $1.720\pm0.005$ |
| FWHM $C3$ (eV) | $0.64\pm0.09$ | $0.47\pm0.02$ |
| Height $a$ ($\times10^4$) | | $2.59\pm0.08$ |
| Position $a$ (eV) | | $1.9816\pm0.0012$ |
| FWHM $a$ (eV) | | $0.114\pm0.004$ |
| $I_0$ ($\times10^4$) | $8.2\pm0.8$ | $4.96\pm0.12$ |
| $E_0$ (eV) | $1.982\pm0.003$ | $2.167\pm0.002$ |
| $S$ | $1.10\pm0.03$ | $0.93\pm0.02$ |
| $E_p$ (eV) | $0.190\pm0.003$ | $0.174\pm0.002$ |
| FWHM (eV) | $0.152\pm0.007$ | $0.151\pm0.004$ |
| $E_{\mathrm{rel}}$ (eV) | $0.209\pm0.007$ | $0.161\pm0.004$ |

yields a good fit to the data, further suggesting that this is a more realistic model for the system. It should be noted that the values of $S$ and $E_p$, 0.93 and 0.174 eV respectively, extracted using model $2a$, are not identical to the values listed in Table I for a spectrum taken at room temperature. This is because a different device, which was fabricated using P3HT from a different batch from Aldrich, was used to obtain these data. It may also be that the extracted data is modified by an imperfect subtraction of the electroabsorption signal due to fluctuations in the relative phases of the signals. The source of this is likely to be variations in the temperature of the sample (on the order of $\pm10$ K) over the period of the experiment (approximately 6 h, in this case). Nevertheless, neither of these observations detract from the essential observation that model $1a$ is incapable of describing the absorption spectrum of P3HT at low temperatures.

Considering the discussion above, one may conclude that model $2a$ more correctly describes the absorption spectrum of rrP3HT. The most striking evidence of this comes from the relaxation energies extracted from each model—model $1a$ yields values that are unphysically high when compared with the values expected from quantum chemical calculations. This, combined with the fact that the lowest-energy fine-structure feature is bleached by a decrease of regioregularity and an increase of temperature (and thus correlated with a decrease in interchain order), can be taken as evidence of the assignment of this feature to an interchain absorption, distinct from the intrachain exciton which is responsible for the higher-energy features. This assignment also explains the independent behavior of the least energetic absorption feature with temperature, regioregularity and solvent which the previous model could not do.

Clearly, it would be instructive to perform a similar analysis on the CMS spectrum of rraP3HT, as published previously.[30] In this case, due to the low mobility of the charge carriers, the charge-induced features are superimposed onto a weak electroabsorption signal. Unfortunately, it is not possible to separate the two signals, as done for the 110-K rrP3HT spectrum,[10] as both signals have phases that are too similar given the magnitude of the noise in the signal. The electroabsorption signal is composed of a sum of the zero-, first-, and second-order derivatives of the absorption spectrum,[45] and this clearly affects the position and intensity of the bleached charge-induced absorption features, rendering accurate analysis impossible.

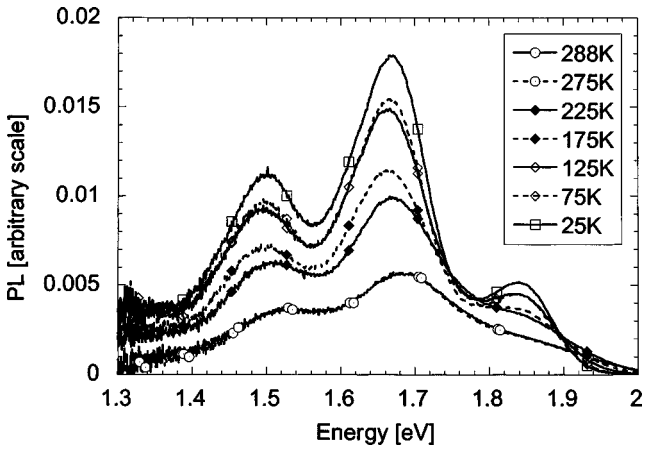


FIG. 6. Temperature dependence of the PL of rrP3HT in units proportional to [photons $\mathrm{s^{-1}\,cm^{-2}\,eV^{-1}}$]; excitation wavelength 488 nm (2.54 eV).

A final point of interest is that the FWHM of the intrachain features (0.17 eV), as extracted from model $2a$, is broader than the FWHM of the interchain feature (0.10 eV), possibly reflecting a different dependence of the inhomogeneous broadening on the local environment of the excitons.

### B. Emission from poly(3-hexylthiophene)

The PL spectrum of rrP3HT excited at 488 nm (2.54 eV) over a range of temperatures, in units proportional to photons $\mathrm{s^{-1}\,cm^{-2}\,eV^{-1}}$, is shown in Fig. 6. At low temperatures three features are observed at 1.84, 1.67, and 1.50 eV. At higher temperatures these features appear to become less intense, broaden, and blueshift. If these spectra are examined while normalized to the height of the nominal 0-0 mode at 1.84 eV (data not shown) one sees that the other features, most notably the nominal 0-1 mode at 1.67 eV, become relatively more intense as the temperature is decreased from 300 to 25 K. What is striking is that these spectra appear to be very similar in functional form to the PL spectra of PPV presented by Ho *et al.*[29] The explanation for the enhanced nature of the 0-1 mode in this system was the presence of a second Franck-Condon progression attributed to emission from an interchain state with an origin corresponding approximately to the energy of the 0-1 mode of an intrachain emission.

In order to fit these emission spectra to a Franck-Condon series the spectra must be divided by $n^3E^3$, where $n$ is the refractive index [shown in Fig. 2(b)], and $E$ is the photon energy, so that the equivalent absorption matrix element (and, thus, Franck-Condon factors) for the transition can be

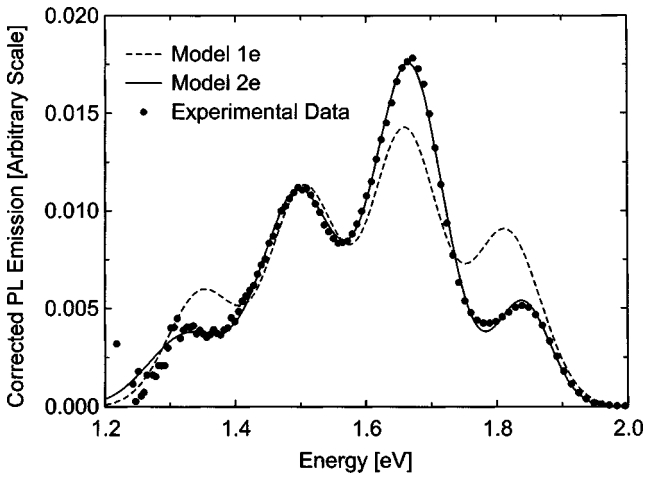


FIG. 7. PL of rrP3HT at 25 K, taken from Fig. 6, after correction for the photonic density of states to allow fitting to Franck-Condon factors. Dashed and solid lines are fits to the data using models $1e$ and $2e$, respectively, as described in the text. Only every seventh point is shown for clarity.

directly modeled. This corrects the emission rate to take into account the photon density of states in the emitting medium which can be inferred from Einstein's $A_{ba}$ and $B_{ab}$ rate coefficients[46–48] or calculated directly from Fermi's golden rule.[49] A first attempt to fit the PL spectrum taken at 25 K is shown in Fig. 7, where the corrected emission rate is plotted against photon energy. The model, similar to model $1a$ discussed in the previous section and hereafter known as model $1e$, is a free fit of a single Franck-Condon series with the 0-0 origin corresponding to the 1.84 eV feature; a single phonon mode, which we have already shown to be a good approximation for rrP3HT, is incorporated into this fit. Again Gaussians were used to fit the features for the same reasons discussed in Sec. III A, although in this case fits using Lorentzians were so poor as to be meaningless. Self-absorption was not a problem as photothermal deflection spectroscopy yielded an absorption of $\sim 10^{-3}$ to $10^{-2}$ lower than the main $\pi$-$\pi^*$ transition in this region.[50,51] Photoinduced self-absorption was also not considered to be a problem as it is likely to be on the scale of $\sim 10^{-3}$.[9] The effect of reflections on the shape of the spectrum were not considered important as most of the emission will come from the surface of the free-standing film. Waveguiding was not present in the device due to the roughness of the film surface, the thinness of the device compared with the wavelength of the light and the geometry of the experiment.

As can be seen, the fit to the corrected emission rate is a poor one, suggesting that the PL spectrum of rrP3HT cannot be considered as an emission from a single electronic state. At this point one may speculate whether the PL spectrum of rrP3HT can be attributed to emission from both an intra and interchain state, in a direct analogy with PPV.[29] This is not unreasonable as rrP3HT can be considered to exhibit greater intra and interchain order than PPV.

Before attempting to fit the spectra using this model, a further assumption is required to extract physically sensible values from the model parameters. This assumption is that the values of $S$ and $E_p$ of the intrachain emission are the same as those observed in absorption. This is not an unreasonable assumption, as many authors have discussed before. Pichler *et al.*[52] experimentally determined that in PPV the phonon modes were softer in emission than absorption by only 10 meV, far less than the FWHM of the features in the PL and CMS spectra. Similar observations for cast poly(2-methoxy, 5-(2′ethyl-hexoxy)-*p*-phenylenevinylene) (MEH-PPV) by Hagler *et al.*[53] showed little or no difference between the phonon energies in absorption and emission; they also observed no difference in the value of $S$. From model $2a$ discussed above, this gives $S=0.7571$ and $E_p=0.1698$ eV for rrP3HT.

Using these two assumptions only, and by allowing the other parameters to vary freely, a very good fit can be obtained (as shown in Fig. 7), yielding sensible physical parameters. This suggests that the PL spectrum of rrP3HT is indeed the sum of two distinct Franck-Condon series and, in a direct comparison with PPV, that the origin may be that of an intrachain and interchain exciton. This model is hereafter known as model $2e$. This successful fit also presents the opportunity to model the temperature dependence of the PL spectra of rrP3HT (assuming that $S$ and $E_p$ are independent of temperature).

The parameters required for model $2e$ are as follows: $I_0$: Total intensity of the intrachain exciton emission. $E_0$: Energy of the intrachain exciton 0-0 feature. $S$: Huang-Rhys factor of the intrachain exciton. $E_p$: Energy of the phonon coupled to the intrachain exciton emission. FWHM: Full width at half-maximum of the inhomogeneously broadened vibronic features. $i_a$: Relative intensity of the interchain emission such that $(I_0 \cdot i_a)$ is the total intensity of the interchain exciton emission. $E_a$, $S_a$, $E_{pa}$, $\mathrm{FWHM}_a$: As above, but for the interchain exciton emission.

The temperature dependences of selected parameters varied in the fit are shown in Fig. 8. Note that the error bars plotted are the standard deviations of the parameters obtained from the fit; although this information is certainly useful, a better estimate of the uncertainty of the parameters can be obtained from the scatter of the surrounding points. From this scatter it can be seen that at temperatures above circa 225 K the spectra need to be interpreted with care as they broaden to such an extent that it is difficult to fit some parameters accurately. A further caveat is that at high temperatures the condition $E_p \gg k_B T$ may not be met; in this case the model for Franck-Condon coupling described above would require modification;[54] however this is not considered important for the analysis discussed here, and many interesting trends in the parameters can be observed.

Although not shown in Fig. 8, $S_a$ and $E_{pa}$ were found to be independent of temperature, as required. This also suggests that the initial assumptions that require $S$ and $E_p$ to be the same in emission and absorption and also that they be independent of temperature are sensible. The mean values of these parameters (taken in the range 25–225 K) are $S_a = 0.714 \pm 0.014$ and $E_{pa} = 0.1710 \pm 0.0013$ eV, yielding a relaxation energy of $0.122 \pm 0.003$ eV. Note that this is slightly

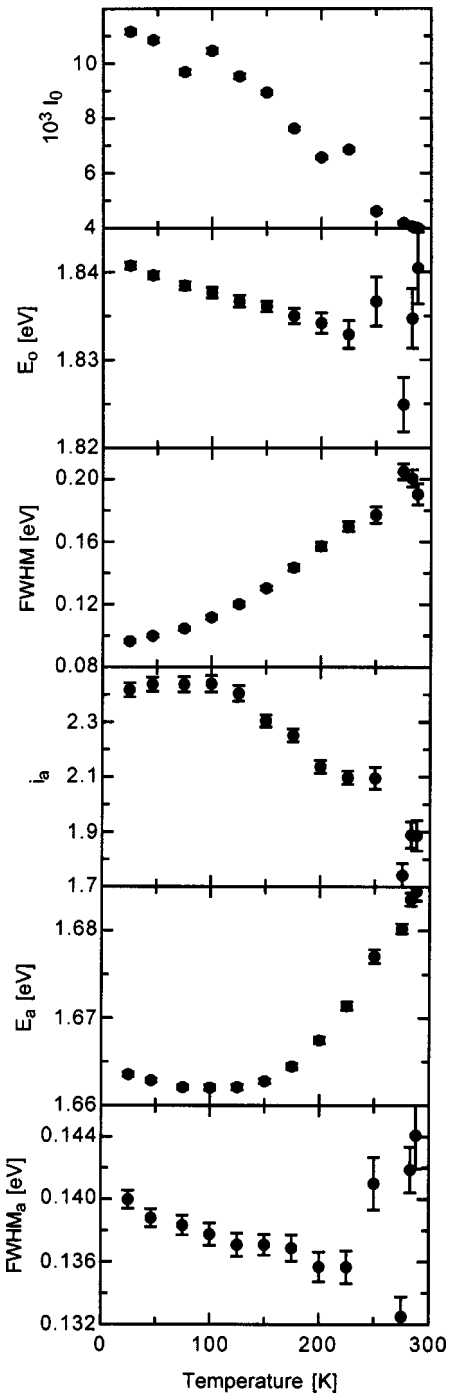


FIG. 8. Temperature dependence of selected parameters yielded by model $2e$ to fit the PL spectra of rrP3HT.

lower than the relaxation energy assumed for the intrachain emission (extracted from the intrachain absorption) of $0.128 \pm 0.04$ eV.

The temperature dependence of $i_a$ is interesting, as this parameter should be strongly influenced by the strength of interchain interactions experienced in the region of the polymer film occupied by the emissive species. At temperatures lower than ~100 K the relative intensity of the interchain exciton is independent of temperature with a value of ~2.4, while above this temperature the parameter decreases almost linearly to a value of ~1.8 at room temperature, reflecting a decrease in the magnitude of interchain interactions and hence in the interchain order. Similarly, the broadening of the intrachain features, as witnessed by the doubling of the FWHM from 0.1 to 0.2 eV as the temperature increases from 0 to 300 K, can be explained by a reduction in intrachain order and hence an increase of inhomogeneous broadening. The increase of $I_0$ with decreasing temperature reflects an increase in the quantum efficiency of the emission process; this is because at lower temperatures thermally activated nonradiative decay routes are quenched.[55]

The temperature dependences of $E_0$, $E_a$, and FWHM$_a$ are curious and at first appear counterintuitive. Although the variations of $E_0$ and $E_a$ with temperature are small, and possibly below the ultimate resolution of the model, given that the scatter and standard deviation of the parameters is much less than the observed variation of the parameters, this raises the likelihood that these trends are real. $E_0$ redshifts with increasing temperature whereas this feature would normally be expected to blue-shift due to the decreasing conjugation length of the chain segments. $E_a$ also appears to redshift to a similar degree up to a temperature of ~100 K; however, at higher temperatures it blueshifts markedly, as expected. The reason for this may be that at low temperatures other effects compete with the effect of increasing conjugation lengths. In inorganic semiconductors the energy gap $E_g$ is well known to increase with decreasing temperatures due to thermal contraction. For example, in Si this is from 1.11 to 1.17 eV as the temperature drops from 300 to 0 K, at an average rate of 200 $\mu$eV/K; this is circa 5 times larger than the rate of 39 $\mu$eV/K between 225 and 25 K observed for rrP3HT. One may expect this rate to be larger for rrP3HT than for Si due to the former's larger thermal expansion coefficient; however, this may be compensated for by the effect of increasing conjugation length with decreasing temperature. Another effect which may also influence $E_0$ and $E_a$ may be a dependence of the Stoke's shift with temperature.

The FWHM of the interchain absorption (FWHM$_a$) appears to decrease with increasing temperature, opposite to the observed broadening of the intrachain exciton; this broadening would be expected if the only influence on FWHM$_a$ was reduced conjugation lengths at high temperatures yielding increased inhomogeneous broadening. One explanation may be that increased interchain interactions at low temperature actually increases the inhomogeneous broadening of the interchain emission due to extra chains participating in the interchain aggregate.

Having used the values of $S$ and $E_p$ from model $2a$, discussed in Sec. III A, it makes sense to try and fit the data assuming values from model $1a$, to wit $S=1.41$ and $E_p = 0.163$ eV. The fits obtained yielded values of $S_a$ and, especially, $E_{pa}$ that were strongly dependent on the temperature of the sample; both $S$ and $E_{pa}$ appeared to increase with decreasing temperature. This suggests that these assumed values of $S$ and $E_{pa}$ are incorrect as a basis for modeling the intrachain emission, as well as yielding $E_{\mathrm{rel}}$ values that are unexpectedly high, and is further evidence for the invalidity of the single intrachain exciton model for absorption in rrP3HT.

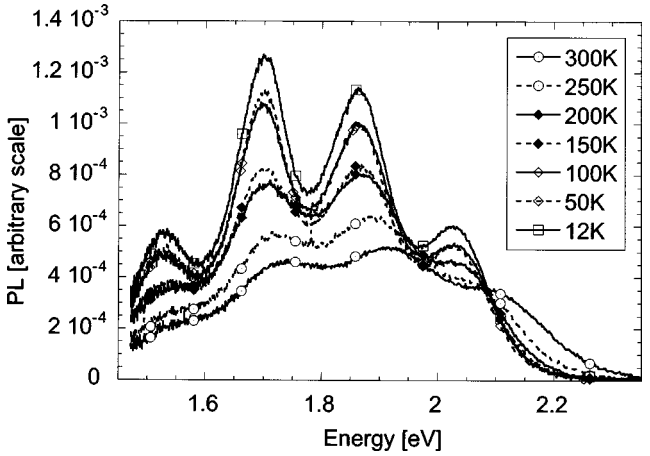


FIG. 9. Temperature dependence of the PL of rraP3HT in units proportional to [photons $s^{-1}\,cm^{-2}\,eV^{-1}$]; excitation wavelength 477 nm (2.60 eV).

A further way to determine the effect of order on the interchain exciton emission process is to vary the regioregularity of the polymer. The temperature dependence of the PL of rraP3HT excited at 477 nm (2.60 eV) was taken, and is shown in Fig. 9. In this case the temperature dependence reveals that the nominal 0–2 mode at ~1.70 eV is enhanced at lower temperatures. This is at a similar energy for the interchain emission observed in rrP3HT and may be evidence of a similar state in rraP3HT.

These spectra can be modeled in a similar manner to that described above by fitting to two Franck-Condon series. Although there is undoubtedly a greater degree of disorder in the film (as witnessed by the CMS spectra and low field-effect mobility),[8] the PL spectrum can still not be modeled by a single Franck-Condon series, indicating that a degree of interchain interaction still exists between the polymer chains. A similar conclusion can be reached by inspection of the CMS spectrum of rraP3HT: there is some absorption in the region of the spectrum attributed to the C3 transition which is the key signature of delocalized polaronic charge carriers; this absorption would not be present in the case of zero interchain interactions.

In order to fit the spectra, a similar assumption for $S$ and $E_p$ to that made for rrP3HT needs to be made for rraP3HT. Unfortunately, the charge-induced signal in the CMS spectrum of rraP3HT is not trivial to separate from the electroabsorption signal (induced by the low-field-effect mobility) present even at room temperature as they have the same phase and so this cannot be a source for this data. Instead, as the polymer is amorphous, one may consider that the Raman spectrum directly probes the regions of the polymer occupied by the excitons as there are no microcrystalline sites for them to diffuse to. This is in direct contrast to the case of rrP3HT where Raman probes the bulk states, whereas CMS probes the microcrystalline regions where both the charge carriers accumulate in an MIS diode and the excitons diffuse to before recombination in a PL experiment. The Raman spectrum of rraP3HT is also shown in Fig. 4, and reveals features that are very similar in position and relative intensity to those observed for rrP3HT. Hence, one may assume that for rraP3HT $E_p = 0.179$ eV, corresponding to the most intense feature in the Raman spectrum.

Unfortunately, it is not possible to estimate a good value of $S$ due to the broad nature of the absorption spectrum (see Fig. 2); however, by only fixing $E_p = 0.179$ eV, good fits can still be made to the PL spectra. The dependence of selected fitted parameters of model $2e$ on temperature is shown in Fig. 10. It should be noted that fits to these spectra did not include the most energetic vibronic feature as significant self-absorption results in a reduced intensity in this region. As for the rrP3HT spectra, the uncertainty in the parameters increases with temperature but, even though the spectra are broader in this case, confidence in the parameters extracted is probably still justified up to a temperature of ~250 K. Broadly speaking, the general trends of all the parameters are similar to those observed for rrP3HT, suggesting that, for the large part, the discussion above for rrP3HT is equally valid for rraP3HT.

Significantly, the value of $i_a$ is a lot lower for rraP3HT compared with that obtained from the PL spectra of rrP3HT. At low temperatures $i_a$ is ~0.35 for rraP3HT and ~2.4 for rrP3HT; this can be considered to be direct evidence of the decrease in interchain interactions and hence in interchain order in rraP3HT with respect to rrP3HT, inhibiting the formation of an interchain emissive state.

The values of $S$, $S_a$, and $E_{pa}$ extracted from these fits appear to be independent of temperature, as required (data not shown). $S$ has an average value of $1.98 \pm 0.4$ (averaged over the range 12–150 K), $S_a = 0.61 \pm 0.4$ (12–150 K), and $E_{pa} = 0.1716 \pm 0.0011$ eV (12–220 K); the relaxation energies of the intra and interchain states are therefore $0.35 \pm 0.07$ and $0.10 \pm 0.07$ eV, respectively. Notably, the values of $S_a$ and $E_{pa}$ and $E_{\mathrm{rel}}$ of the interchain exciton are very similar to the values extracted from the PL spectra of rrP3HT. It is also the case that while $E_0$ differs by 0.2 eV between the two polymers at low temperature, $E_a$ differs by only 0.04 eV. Not only does this reveal that the two different emissive states are affected differently by local order, it also suggests that the energetics of interchain exciton are almost independent of polymer regioregularity, in contrast to the intrachain exciton.

As a final point, it is worth examining previously published PL spectra of PT. Before the advent of highly regioregular P3HT, polythiophene films were highly disordered and, as a result, the PL spectra should exhibit very low or even no contributions from an interchain emissive state. Kaneto *et al.*[56] presented the PL spectrum of such an electrochemically synthesized polymer in 1984. Inspection of the spectrum reveals that none of the vibronic features appear to be enhanced in the same way that the nominal 0–1 feature in the PL spectrum of rrP3HT or the nominal 0–2 feature of the rraP3HT PL spectrum presented here are. Indeed, the features appear to be well modeled by the Franck-Condon parameters attributed to intrachain emission in rrP3HT above, namely, $S \sim 0.8$. Shinar *et al.* also published PL spectra of PT pressed into KBr pellets[20] which showed four features separated by 0.182 eV, suggesting a single phonon mode; inspection of the spectrum suggests $S \sim 1$. This strongly suggests that the PL of this polymer can be modeled by a single in-

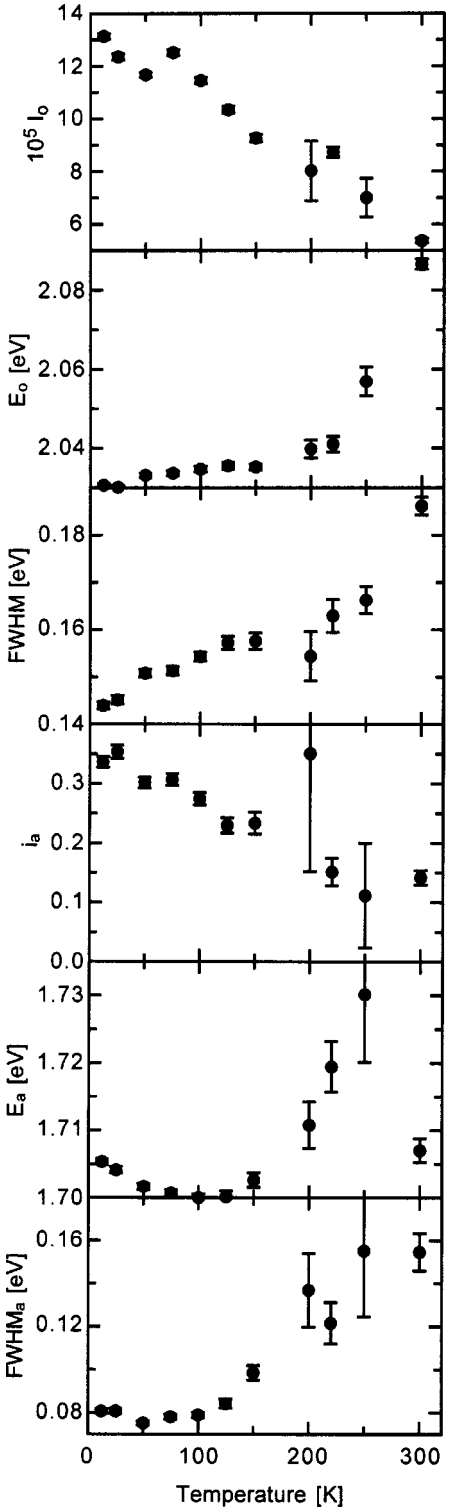


FIG. 10. Temperature dependence of selected parameters yielded by model $2e$ to fit the PL spectra of rraP3HT.

trachain Franck-Condon progression coupled to a single phonon mode. A further method of reducing the magnitude of interchain interchain interactions is to substitute bulky side groups onto the thiophene backbone. Ruseckas *et al.*[23] performed PL on such a polymer and obtained a single Franck-Condon progression with $S=0.6$ (cf. $S$ for the intrachain exciton reported here for rrP3HT) and $E_p=0.175$ eV. This apparent absence of a second emissive state in PT films with little or no interchain interactions can be seen as a final piece of evidence for an interchain emissive state in rrP3HT.

The model proposed here for the emission from substituted PT is different from those reported previously. Sakurai *et al.*[22] suggested that the absorption was due to an intrachain exciton Franck-Condon coupled to a single phonon with $S=2$, whereas the PL was due to a similar exciton with $S=3$. Ruseckas *et al.*[24] proposed a different model whereby the emission was due to an aggregate state and that the exciton, again coupled to a single phonon mode ($E_p \sim 0.165$ eV), exhibited purely interchain characteristics with $S\sim 2$. The detailed modeling of the PL spectrum of rr and rraP3HT discussed above shows that these models are incorrect as two Franck-Condon progressions coupled to a single phonon are required to accurately describe the PL spectrum.

### C. Further characterization of the electronic states of P3HT

Site-selective PL measurements can be useful in determining the exact relationship between absorption features and the emission they produce by varying the pump beam energy. The PL of rrP3HT was measured at 12 K upon excitation at 633 and 497.5 nm (1.96 and 2.49 eV), that is into the low energy tail of the interchain absorption feature and the middle of the intrachain absorption, respectively. (Note that at 12 K, the absorption spectrum shown in Fig. 2 undergoes a thermochromic redshift).[10] Little difference was observed between the 633- and 497.5-nm excited spectra, although the former spectrum did appear to exhibit characteristics suggesting emission from a slightly more disordered environment than those observed in the latter. Unfortunately, due to the broad nature of the intrachain absorption and the thermochromic redshift of the spectrum from room temperature, illumination at 1.96 eV does not purely excite the interchain absorption, however it is interesting to note that a similar result is obtained for poly(9,9-dioctylfluorene) when the PL obtained by exciting an interchain absorption feature is seen to be comparable to the PL obtained by exciting the broad intrachain absorption band.[57] The slight differences in the rrP3HT spectra are probably due to the localization threshold of rrP3HT being higher than 1.96 eV, as described by Harrison *et al.*[58]

As the interchain emission shows structured vibronic features, both for P3HT and PPV,[29] it is reasonable to ask whether the interchain absorption exhibits vibronic structure, as opposed to the single Gaussian absorption feature modelled above in model $2a$. Many attempts to fit the CMS spectrum of P3HT were made by selecting a variety of values for $S_a$ and $E_{pa}$, including those extracted from the PL spectra. None of the attempts yielded reasonable fits to the data, indeed when $S_a$ and $E_{pa}$ were allowed to become free parameters in the fits, a value of $6\times 10^{-2}$ was obtained for $S_a$, which is effectively the single Gaussian assumed in model $2a$. This suggests that the interchain excited state is only loosely bound, such that only one bound vibronic state occurs in the potential energy curve of the excited state. The continuum of excited states of the electron, reached by ex-

citing the exciton out of the bound state, will not show up in the absorption spectrum of P3HT if these states are not strongly coupled to the ground state, $S_0$. This is feasible if one considers the small overlap between the wavefunctions of a delocalized and highly localized state.

The usual model for describing intermolecular interactions invokes the concept of *H* and *J* aggregates of dipole-coupled chains.[34,37] *H* aggregates are formed when the molecules adopt a cofacial structure whereas an end to end formation results in a *J* aggregate; *H* aggregates typically result in a blueshift of the absorption spectrum whilst *J* aggregates result in a redshift. In the case of P3HT the molecules are cofacial, and hence analogous to *H* aggregates, and yet the interchain absorption is at a lower energy than the intrachain absorption. Manas and Spano[59] and Cornil *et al.*[28,36] performed calculations on *H* aggregates of conjugated chains at a fixed interchain distance whilst varying the length of the chains. They showed that as the chain length was increased from short chains to longer ones more closely imitating a polymer the splitting of the dipole-coupled energy levels at first increased before becoming constant at a chain length of about ten conjugated units and then decreasing as the chains became longer. This would show up as an initial blueshift of the main absorption as the degree of order in a polymer film increases before redshifting. One may consider P3HT as being modeled by an intrachain exciton in the intermediate regime and an interchain exciton in the more ordered regime. This situation, however, does not appear to correctly model the P3HT system as the analysis discussed in this paper shows that the energy of the interchain features are not strongly dependent on any variable that controls the degree of interchain interactions. The conclusion is that the effect of interchain interactions on the electronic structure of P3HT cannot be explained by the dipole-coupled *H* and *J* aggregate models. It may be that the absorption and emission features are due to transitions between states previously unconsidered by quantum chemical calculations, missed due to the inherent approximate nature of the technique. Ultrafast, femtosecond spectroscopy may be a useful tool for studying the details of the formation of excitons in this material.

One should also consider why the new interchain absorption feature is not observed in the spectra of other similar conjugated polymers. PPV is a system that is very similar to P3HT as it incorporates conjugated rings along the main polymer backbone. The difference is that PPV (and its soluble derivatives) generally forms amorphous films which suggests low intrachain interactions. Some groups have managed to order PPV, however this has always resulted in reduced interchain interactions. Pichler *et al.* reported a PPV that exhibited a high intrachain order.[52] This was determined by the sharpness and distribution of the optical features in absorption and emission and also from electron diffraction analysis. Conversely, the electron-diffraction data also showed that the interchain coherence length had reduced from 65 to 45 Å, further decreasing the strength of interchain interactions affecting the absorption spectrum in a polymer where they were already weak. Other efforts to increase the degree of order in PPV derivative films included blending the polymer in an inert matrix and drawing to a high ratio. Whilst this did achieve the effect of increasing the intrachain order, the inert matrix greatly reduced the interchain interactions between the PPV molecules.[53,60,61]

It is important to stress that while the UV–vis absorption spectrum samples all chain segments, the PL spectrum only samples the most ordered states so it is possible for the two spectra to exhibit features characteristic of differing degrees of interchain order. This would explain the presence of interchain emission but not of interchain absorption in PPV. As a last point one should note that when PPV does form ordered regions it is in a monoclinic herringbone conformation,[62] not in the cofacial manner of P3HT, meaning that the wave functions on different chains will mix differently when interacting. It is for these reasons that the absorption spectrum of PPV is liable to be different from that of P3HT and will certainly exhibit less interchain features.

Polydiacetylenes (PDAs) are a class of conjugated polymer that form single crystals and so have the potential to exhibit increased interchain effects. In these materials, however, the interchain distance is large compared with P3HT (3.8 Å) and interchain interactions decrease approximately exponentially with interchain distance. Typical interchain distances are 7.5 Å for poly[2, 4-hexadiyn-1, 6-diol-bis(p-toluene sulfonate)] (PDA-TS) (Ref. 63) and 5.5 Å for poly{5, 7-dodecadiyene-1, 2-diol bis [((4-butoxycarbonyl)methyl)-urethane]} (4BCMU).[64] We note that PDA-TS exhibits a splitting of the 0-0 excitonic absorption feature below 195 K which is caused by the interaction between its side chains despite the large interchain distance. This is caused by a phase transition, driven by the aromatic side chains, and reduces the symmetry of the crystal. This process results in inequivalent PDA chains per unit cell and means that the splitting in the absorption spectrum is due to Davydov splitting rather than enhanced electronic interaction. This process is not present in P3HT as the side chains do not drive a further phase transition other than to increase the inter and intrachain ordering in the solid state.

As a final point it should be noted that the chemical structures of PDAs are significantly different from P3HT in that they are a straight chain polymer incorporating double and triple bonds in their backbones. This means any mixing of states on neighboring chains is likely to produce a different effect from that discussed in this paper.

A comparison with regioregular head-to-tail oligoalkylthiophenes is also difficult, as these materials have only recently been fabricated to a high purity and only solution absorption spectra have been reported to date.[65–67] An earlier attempt to measure the solid state absorption spectrum of 3-alkyl substituted terthiophene reported a broad spectrum whereby only the peak absorption was resolvable suggesting large interchain disorder.[68]

A further family of conjugated polymer that exhibits a large degree of intra-chain order is ladder type poly(paraphenylene) (LPPP). Although the bridging segments of the chain force the polymer backbone into a planar configuration, the interchain packing is amorphous, due to the nonplanar solubilizing side-chains.[69] Significantly, however, Köhler *et al.*[70] revealed that LPPP displays an absorption at 2.25 eV that is redshifted by ~0.5 eV from the main, well-resolved, solid-

state, intrachain absorption. This was first identified in the photovoltaic properties of the polymer, and as a result a weak interchain absorption was also identified. It may be that this is the equivalent of the interchain absorption feature identified in P3HT in this paper.

As a final point it is worth considering the comparison between rrP3HT and single crystalline sexithiophene (6T), the absorption spectrum for which has recently been reported. Weiser and Möller[71] showed that polariton effects are present in the absorption and reflection spectra of single crystalline 6T and that this modified the assignment of spectral features. It is important to note that this cannot be the reason for any features in the spectra of P3HT. Although P3HT exhibits highly ordered domains embedded in an amorphous matrix, these domains are not single crystalline, and therefore polariton features are not expected in the spectrum of P3HT. This interpretation can be made for several reasons: (1) The charge carriers in P3HT are not quasi-free particles but instead are localized by disorder and exhibit polaronic characteristics, albeit quasi-two-dimensional ones; (2) Improved processing of P3HT can still increase the field-effect mobility and the delocalization of the polaronic charge carriers—this would not be possible if the polarons were sited in a single crystalline environment. (3) X-ray analysis reveals that not only are the highly-ordered domains not single crystalline, but that they are small at about 10 nm in size. This is a very short coherence length for the coupled interaction between light and the polarization of the polymer chains.

### D. Probing the effect of disorder with CMS

As we showed in a previous paper,[10] dc bias-dependent CMS spectra of rrP3HT are able to probe states of differing order. Briefly, when a MIS diode is biased at the onset of accumulation the first charges will be placed in the least energetic unoccupied states, corresponding to the most ordered states. As the device is biased further into accumulation the extra charge will be placed in states of higher and higher energy, and the CMS spectrum will, in turn, reflect the increasing disorder in these states. In terms of the charged features, as states of increasing order are probed the intensity of the $C1$ (the near-infrared polaronic feature not shown in the CMS spectra presented in this paper) and $C3'$ transitions increase while $C3$ becomes less intense and red shifts. The bleaching signal also evolves to reflect these changes and the fine structure becomes less well resolved.

As we are now able to assign all the features in the CMS spectrum of P3HT correctly, it is also possible to model the dc bias-dependent spectra such that a more quantitative analysis of the effect of disorder can be performed. Figure 11 shows the bias dependence data of rrP3HT taken at room temperature with a modulation frequency of 37 Hz, the $+10$ V spectrum was taken first, and the $-10$ V spectrum last, although qualitatively no difference is observed when this direction is reversed. Both the bleached absorption features and the subgap polaronic features can be modeled, and they shall be discussed separately in that order.

As can be seen from Fig. 3, the biggest discrepancy between the fit of model 2 and the experimental data is at low

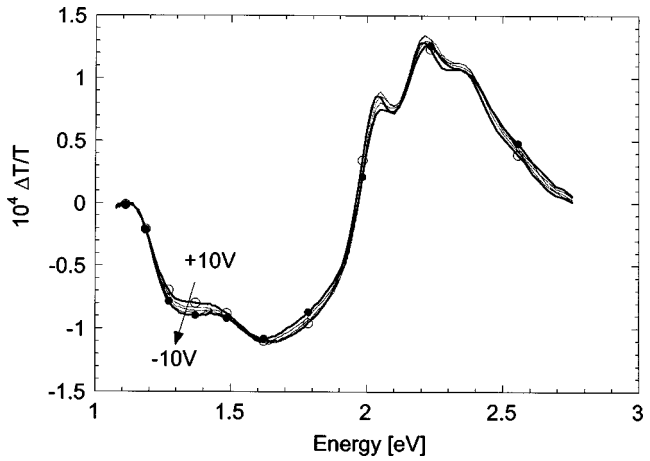


FIG. 11. Bias dependence of the room-temperature CMS spectrum of rrP3HT in the visible region, spectra taken in the order shown by the arrow. The modulation frequency was 37 Hz. Solid markers: $-10$-V spectrum; hollow markers: $+10$-V spectrum; intermediate scans in 5-V steps are shown in gray.

energies, $<\sim 1.4$ eV around the region of the $C3'$ polaronic feature. This discrepancy is the source of a large fraction of the uncertainty in the fit parameters, but since this feature does not affect the values of the parameters required to model the bleaching spectrum the fits to model the bleached absorption features were performed from 1.55 eV onwards, yielding uncertainties in the parameters that were a factor of approximately three lower than shown in Table I.

The result of the modeling is shown in Figs. 12(a) and 12(b), where the parameters required to fit the bleached absorption features (inter and intrachain, respectively) are plotted against applied dc bias. The following trends are clearly observed as the bias is swept from the onset of accumulation deeper into accumulation (from $+10$ to $-10$ V).

(1) The intensity of the interchain absorption feature decreases from circa 1.05 to $0.8\times10^{-4}$.

(2) The energy of the first absorption peak appears to be largely independent of the applied bias.

(3) $E_0$ (the 0-0 transition of the intrachain exciton) blueshifts by 6 meV.

(4) The interchain and intrachain features broaden.

(5) The Huang-Rhys parameter decreases.

(6) The phonon energy increases.

These trends, although small, are repeatable and can be observed for all poly(3-alkylthiophenes). Observations (1), (3), (4) and (6) are consistent with the degree of order associated with the states responsible for the CMS spectrum becoming more disordered as the bias is swept from the onset of accumulation further into accumulation. Observation (2) is consistent with the PL data, that show the interchain emission features are affected by the degree of disorder to a lesser extent than the intrachain features.

Observation (5) is, at first sight, puzzling. As the degree of disorder increases many researchers have already shown that charge carriers become more localized on a chain,[72–75] this is because disorder reduces interchain interactions and causes greater lattice and electronic relaxation. This, in turn, should be reflected in an increase in $\Delta Q$ as the exciton forms

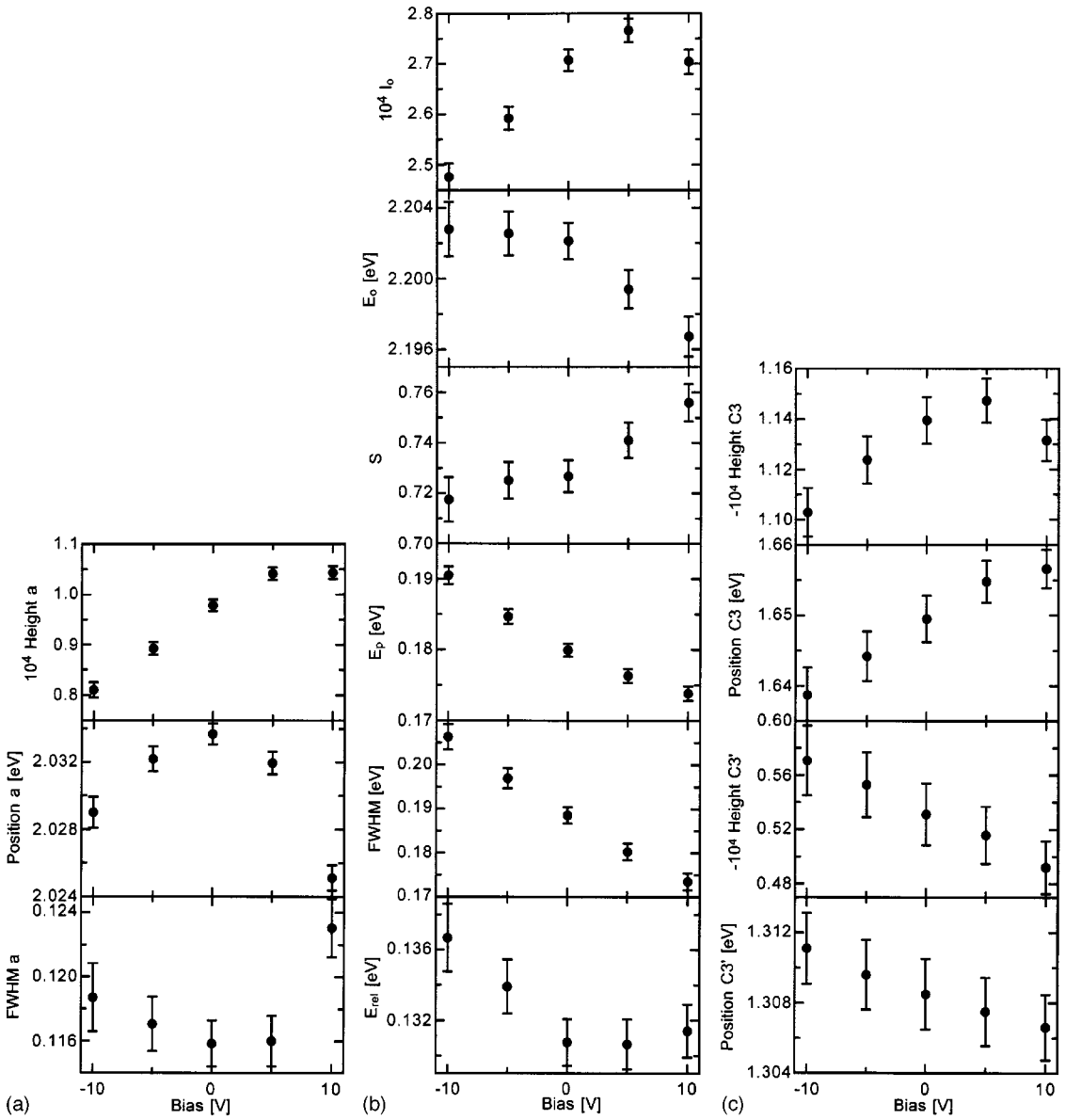


FIG. 12. Bias dependence of the parameters required to fit the CMS spectra of rrP3HT, shown in Fig. 11. (a) Bleached interchain absorption feature. (b) Bleached intrachain absorption features. (c) Subgap polaronic features.

which leads to the conclusion that $S$ should also increase, assuming $E_p$ is constant [from Eq. (3)]. Observation (5) is inconsistent with this; however, Fig. 12(b) shows that $E_p$ is not independent of applied bias, which offers a way out of this paradox if one considers the relaxation energy of the absorption. Intuitively, one might expect $E_{\mathrm{rel}}$ to increase as the amount of disorder increases because the molecule has to increase the electronic and lattice distortion in order to accept the presence of an exciton on a chain. This is exactly what is shown in Fig. 12(b), showing that the initially unexpected trend exhibited by $S$ does not indicate a flaw in the model.

Figure 12(c) shows the dependence of the polaronic subgap features on the applied dc bias, as extracted by modeling the full CMS spectrum presented in Fig. 11. Although the fits to the sub-gap polaronic features are not as accurate as the fits to the bleaching features, many interesting trends can be picked out from the data. Certainly, the increased relaxation of the charge carrier as states of greater disorder are probed are picked up in terms of the blue-shift and increased intensity of $C3'$ and the redshift and reduced intensity of $C3$.[30] The fits to this data are not good enough to pick up a dependence of the FWHM of the features on applied bias (data not shown).

A close inspection of the data shown in Fig. 12, and in particular the points at $+10$ V, shows that some of the parameters show a deviation from the trend set by the other points at more negative biases. It is highly likely that at this bias a small signal due to electroabsorption is present and if so this will slightly distort the pure bleaching signal. This deviation from the expected trend can also be seen on close inspection of the charge-induced features in Fig. 11, most prominently in the position and shape of the $C3$ feature.

The ability to accurately extract the integrated intensity of the features allows the oscillator strength of the features to be calculated. It can be shown that in accumulation the magnitude of the CMS spectrum of the sub-gap, charge-induced features can be written as[33]

$$\frac{\Delta T}{T} = -\frac{\sigma}{eA} C \Delta V, \tag{5}$$

where $\sigma$ is the absorption cross section, $e$ is the charge of an electron, $A$ is the active area of the MIS diode, $C$ is the capacitance of the insulator, and $\Delta V$ is the peak to peak a.c. modulation voltage. The optical cross section can be written as the molar extinction coefficient, $\varepsilon$, using the definition

$$\sigma = \frac{1000 \ln(10)}{N_A} \varepsilon \tag{6}$$

where $N_A$ is Avogadro's constant. The oscillator strength of a transition, $f$, is defined as[34]

$$f = \frac{4.39 \times 10^{-9}}{n_0} \int \varepsilon(\bar{\nu}) d\bar{\nu}, \tag{7}$$

where $\bar{\nu}$ is the wave number of the transmitted light and the integration is performed over the whole optical width of the transition. By substituting Eqs. (5) and (6) into Eq. (7) and changing the units of integration to eV, the following can be obtained:

$$f = 9.276 \times 10^{17} \frac{eA}{n_0 C \Delta V} \int -\frac{\Delta T}{T} d\nu, \tag{8}$$

where $\nu$, the photon energy, is in units of eV. The active area of our MIS diodes is $4 \times 5\ \mathrm{mm}^2$, $n_0$ can be obtained from ellipsometry (1.91 for the $C3'$ transition and 1.97 for $C3$), $C$ is 3.55 nF, and $\Delta V$ is 2 V. The area of one of the gaussian features in the fits to the CMS spectra can be shown to be

$$\int -\frac{\Delta T}{T} d\nu = -\mathrm{Height} \times \mathrm{FWHM} \times \left( \frac{\pi}{\ln 16} \right)^{1/2}$$
$$= -1.064 \times \mathrm{Height} \times \mathrm{FWHM} \tag{9}$$

where Height and FWHM are parameters extracted from the fits. Using Eqs. (8) and (9), the oscillator strengths of the polaronic transitions observed in the +5-V CMS spectrum shown in Fig. 11 are calculated to be $f(C3') = (2.08 \pm 0.12) \times 10^{-3}$ and $f(C3) = (1.33 \pm 0.08) \times 10^{-2}$, with relative intensities of 1:6.4 (cf. a value of 6.7 reported earlier, extracted from less accurate modeling).[10] Most of the uncertainty comes from the capacitance (which is affected by hysteresis) and $n_0$ which is not constant over these broad transitions. By incorporating these values into a suitable theoretical framework[30] an estimate of the coherence length of the polaronic delocalisation may be possible. This, in turn, may allow a fuller characterization of the degree of order in the microcrystalline domains of P3HT. The bias dependence of the height and FWHM of the polaronic features extracted from the CMS spectra, shown in Fig. 12(c), will also allow an estimate of the range of coherence lengths probed with this technique.

## IV. CONCLUSIONS

Whereas the absorption spectrum of PT has previously been attributed to a single intrachain exciton coupled to a single phonon mode, we have shown that this model is too simplistic in highly ordered rrP3HT. The increased interchain interactions in this polymer result in a characteristic absorption feature at the onset of the $\pi$-$\pi^*$ transition that, until now, has been misinterpreted as the 0-0 vibronic origin of the absorption of an intrachain exciton. The intensity of the new absorption feature has been shown to be correlated with other physical variables, such as temperature and regioregularity, which alter the degree of interchain order in the microcrystalline domains of P3HT, resulting in us assigning this feature to an interchain process. We assign the 0-0 origin of the intrachain exciton to the next most energetic fine structure feature in the absorption spectrum. As a result of this reassignment we have shown that the relaxation energy of the first intrachain singlet excited state in rrP3HT is ~0.12–0.13 eV, compared with ~0.23 eV calculated from the previous model; this revised figure is in far better agreement with the quantum chemical calculations of Cornil and co-workers.[25–28,35,36]

The emission spectrum of rrP3HT also exhibits interchain emission, similar to that already shown in PPV.[29] This has been confirmed by modeling the temperature dependent PL spectra of rr and rraP3HT and extracting the parameters relevant to both the inter and intrachain emission. As for the case of absorption, we can monitor and correlate the changes in the emission spectrum by varying several physical parameters (such as temperature of the solid film and regioregularity of the polymer) that change the local order in the regions from where the emission originates.

The discussion presented in this paper clearly shows that the previous model of absorption and emission, which correctly models disordered polymers, is simply not consistent with the characteristic spectra of P3HT and, therefore, that a new model is required. The revised model proposed is not only consistent with these established models, but also self-consistent in that it accurately describes the absorption and emission processes in P3HT together. Even if one were to attempt to erroneously force the old model to describe the absorption of P3HT (which only fortuitously yields a reasonable fit at room temperature, see Figs. 3 and 5) this would then result in a completely false picture of the emission. This is easily demonstrated by using parameters required to fit the absorption to fit the emission, as discussed in Sec. III B the results do not match. This demonstrates the robustness of the analysis presented here.

Both the absorption and emission spectra reveal that many characteristics of the interchain features are less dependent on disorder than the intrachain features. The energy of the 0-0 feature, the Huang-Rhys parameter and the phonon energy of the interchain emission are very similar in both rr and rraP3HT whereas they are quite different for the intrachain

emission. Further, a reduced relaxation energy for the interchain emission is also observed, relative to the intrachain emission. These are all experimental facts that need to be explained by any future theory of interchain aggregate states in P3HT.

By fitting the dc bias-dependent CMS spectra of rrP3HT, using this model of the absorption processes, we have shown that the energy of the phonon mode coupled to the intrachain exciton exhibits dispersion in that it softens as the degree of intrachain order increases. The improved modeling of the CMS spectrum of rrP3HT also allows better characterization of the polaronic sub-gap absorption features. Oscillator strengths of the most energetic features, labeled $C3'$ and $C3$,[30] are found to be $2.08\times10^{-3}$ and $1.33\times10^{-2}$, respectively. Within the framework of a suitable model this information may be useful in extracting a correlation length of the quasi-two-dimensional polaronic charge carriers and thus yield a more quantitative picture of the degree of order in rrP3HT.

## ACKNOWLEDGMENTS

This work was supported by the NEDO International Joint Research Program, 99MB1 Nonlinear Excitations in Molecular Electronic Materials: Detection, Control and Device Application.

*Email address: p.j.brown.96@cantab.net
†Email address: hs220@phy.cam.ac.uk

[1] R. D. McCullough and R. D. Lowe, J. Chem. Soc. Chem. Commun. **1992**, 70.
[2] T. A. Chen, X. M. Wu, and R. D. Rieke, J. Am. Chem. Soc. **117**, 233 (1995).
[3] R. S. Loewe, S. M. Khersonsky, and R. D. McCullough, Adv. Mater. **11**, 250 (1999).
[4] Z. Bao, A. Dodabalapur, and A. J. Lovinger, Appl. Phys. Lett. **69**, 4108 (1996).
[5] H. Sirringhaus, N. Tessler, and R. H. Friend, Science **280**, 1741 (1998).
[6] H. Koezuka, A. Tsumura, and T. Ando, Synth. Met. **18**, 699 (1987).
[7] E. J. Samuelsen and J. Mardalen, in *Handbook of Organic Conductive Polymers*, edited by H. S. Nalwa (Wiley, Weinheim, 1997), Vol. 3, Conductive Polymers: Spectroscopy and Physical Properties, pp. 100–106.
[8] H. Sirringhaus *et al.*, Nature (London) **401**, 685 (1999).
[9] R. Österbacka, C. P. An, X. M. Jiang, and Z. V. Vardeny, Science **287**, 839 (2000).
[10] P. J. Brown, H. Sirringhaus, M. Harrison, M. Shkunov, and R. H. Friend, Phys. Rev. B **63**, 125204 (2001).
[11] M. Sundberg, O. Inganäs, S. Stafstrom, G. Gustafsson, and B. Sjogren, Solid State Commun. **71**, 435 (1989).
[12] J. J. Apperloo, R. A. J. Janssen, M. M. Nielsen, and K. Bechgaard, Adv. Mater. **12**, 1594 (2000).
[13] H. Tachibana, N. Hosaka, and Y. Tokura, Macromolecules **34**, 1823 (2001).
[14] W. R. Salaneck, O. Inganäs, B. Themans, J. O. Nilsson, B. Sjogren, J. E. Osterholm, J. L. Brédas, and S. Svensson, J. Chem. Phys. **89**, 4613 (1988).
[15] O. Inganäs, W. R. Salaneck, J. E. Osterholm, and J. Laakso, Synth. Met. **22**, 395 (1988).
[16] O. Inganäs, G. Gustafsson, W. R. Salaneck, J. E. Osterholm, and J. Laakso, Synth. Met. **28**, C377 (1989).
[17] W. R. Salaneck, O. Inganäs, J. O. Nilsson, J. E. Osterholm, B. Themans, and J. L. Brédas, Synth. Met. **28**, C451 (1989).
[18] K. Iwasaki, H. Fujimoto, and S. Matsuzaki, Synth. Met. **63**, 101 (1994).
[19] M. Theander, M. Svensson, A. Ruseckas, D. Zigmantas, V. Sundstrom, M. R. Andersson, and O. Inganäs, Chem. Phys. Lett. **337**, 277 (2001).
[20] J. Shinar, Z. Vardeny, E. Ehrenfreund, and O. Brafman, Synth. Met. **18**, 199 (1987).
[21] J. Cornil, D. Beljonne, Z. Shuai, T. W. Hagler, I. Campbell, D. D. C. Bradley, J. L. Brédas, C. W. Spangler, and K. Mullen, Chem. Phys. Lett. **247**, 425 (1995).
[22] K. Sakurai, H. Tachibana, N. Shiga, C. Terakura, M. Matsumoto, and Y. Tokura, Phys. Rev. B **56**, 9552 (1997).
[23] A. Ruseckas, E. Namdas, M. Theander, M. Svensson, A. Yartsev, D. Zigmantas, M. R. Andersson, O. Inganäs, and V. Sundström, Synth. Met. **119**, 603 (2001).
[24] A. Ruseckas, E. B. Namdas, T. Ganguly, M. Theander, M. Svensson, M. R. Andersson, O. Inganäs, and V. Sundström, J. Phys. Chem. B **105**, 7624 (2001).
[25] J. Cornil, D. Beljonne, C. M. Heller, I. H. Campbell, B. K. Laurich, D. L. Smith, D. D. C. Bradley, K. Mullen, and J. L. Brédas, Chem. Phys. Lett. **278**, 139 (1997).
[26] J. Cornil, D. Beljonne, and J. L. Brédas, in *Electronic Materials: The Oligomer Approach*, edited by K. Müllen and G. Wegner (Wiley-VCH, Chichester, 1998), pp. 432–447.
[27] J. Cornil, D. Beljonne, V. Parente, R. Lazzaroni, and J. L. Brédas, in *Handbook of Oligo and Polythiophenes*, edited by D. Fichou (Wiley-VCH, Chichester, 1998), pp. 317–360.
[28] J. Cornil, D. A. Dossantos, X. Crispin, R. Silbey, and J. L. Brédas, J. Am. Chem. Soc. **120**, 1289 (1998).
[29] P. K. H. Ho, J. S. Kim, N. Tessler, and R. H. Friend, J. Chem. Phys. **115**, 2709 (2001).
[30] D. Beljonne, J. Cornil, H. Sirringhaus, P. J. Brown, M. Shkunov, R. H. Friend, and J. L. Bredas, Adv. Funct. Mater. **11**, 229 (2001).
[31] M. Cardona, *Modulation Spectroscopy* (Academic, London, 1969).
[32] M. G. Harrison, R. H. Friend, F. Garnier, and A. Yassar, Synth. Met. **67**, 215 (1994).
[33] P. J. Brown, Ph.D. thesis, University of Cambridge, 2000.
[34] M. Pope and C. E. Swenberg, *Electronic Processes in Organic Crystals* (Clarendon, Oxford, 1982).
[35] J. L. Bredas, J. Cornil, D. Beljonne, D. Dos Santos, and Z. G. Shuai, Acc. Chem. Res. **32**, 267 (1999).
[36] J. Cornil, D. Beljonne, J. P. Calbert, and J. L. Brédas, Adv. Mater. **13**, 1053 (2001).
[37] G. Louarn, J. Y. Mevellec, J. P. Buisson, and S. Lefrant, Synth. Met. **55**, 587 (1993).
[38] G. Louarn, M. Trznadel, J. P. Buisson, J. Laska, A. Pron, M.

Lapkowski, and S. Lefrant, J. Phys. Chem. **100**, 12 532 (1996).
[39] J. T. Lopez Navarrete and G. Zerbi, J. Chem. Phys. **94**, 957 (1991).
[40] J. T. Lopez Navarrete and G. Zerbi, J. Chem. Phys. **94**, 965 (1991).
[41] B. Tian, G. Zerbi, R. Schenk, and K. Mullen, J. Chem. Phys. **95**, 3191 (1991).
[42] B. Tian, G. Zerbi, and K. Mullen, J. Chem. Phys. **95**, 3198 (1991).
[43] B. Tian and G. Zerbi, J. Chem. Phys. **92**, 3886 (1990).
[44] B. Tian and G. Zerbi, J. Chem. Phys. **92**, 3892 (1990).
[45] M. G. Harrison, S. Moller, G. Weiser, G. Urbasch, R. F. Mahrt, H. Bassler, and U. Scherf, Phys. Rev. B **60**, 8650 (1999).
[46] P. W. Atkins and R. S. Friedman, *Molecular Quantum Mechanics* (Oxford University Press, Oxford, 1997).
[47] B. H. Brandsen and C. J. Joachain, *Introduction to Quantum Mechanics* (Wiley, Harlow, 1994).
[48] S. J. Strickler and R. A. Berg, J. Chem. Phys. **37**, 814 (1962).
[49] L. E. Ballentine, *Quantum Mechanics* (Prentice-Hall International, London, 1990).
[50] H. Sirringhaus, N. Tessler, D. S. Thomas, P. J. Brown, and R. H. Friend, in *Advances In Solid State Physics 39*, edited by B. Kramer (Vieweg, Wiesbaden, 1999), pp. 101–110.
[51] D. S. Thomas, Ph. D. thesis, University of Cambridge, 1999.
[52] K. Pichler, D. A. Halliday, D. D. C. Bradley, P. L. Burn, R. H. Friend, and A. B. Holmes, J. Phys.: Condens. Matter **5**, 7155 (1993).
[53] T. W. Hagler, K. Pakbaz, K. F. Voss, and A. J. Heeger, Phys. Rev. B **44**, 8652 (1991).
[54] V. Seshadri and V. M. Kenkre, Phys. Rev. A **17**, 223 (1978).
[55] N. J. Turro, *Modern Molecular Photochemistry* (University Science Books, Sausalito, CA, 1991).
[56] K. Kaneto, Y. Kohno, and K. Yoshino, Solid State Commun. **51**, 267 (1984).
[57] M. Grell, D. D. C. Bradley, X. Long, T. Chamberlain, M. Inbasekaran, E. P. Woo, and M. Soliman, Acta Polym. **49**, 439 (1998).
[58] N. T. Harrison, D. R. Baigent, I. D. W. Samuel, R. H. Friend, A. C. Grimsdale, S. C. Moratti, and A. B. Holmes, Phys. Rev. B **53**, 15 815 (1996).
[59] E. S. Manas and F. C. Spano, J. Chem. Phys. **109**, 8087 (1998).
[60] E. K. Miller, C. Y. Yang, and A. J. Heeger, Phys. Rev. B **62**, 6889 (2000).
[61] E. K. Miller, C. J. Brabec, H. Neugebauer, A. J. Heeger, and N. S. Sariciftci, Chem. Phys. Lett. **335**, 23 (2001).
[62] V. Enkelmann, in *Electronic Materials: The Oligomer Approach*, edited by K. Müllen and G. Wegner (Wiley-VCH, Chichester, 1998), pp. 313–316.
[63] M. J. Nowak, G. J. Blanchard, G. L. Baker, S. Etemad, and Z. G. Soos, Phys. Rev. B **41**, 7933 (1990).
[64] G. Weiser and A. Horvath, Chem. Phys. **227**, 153 (1998).
[65] T. Kirschbaum, R. Azumi, E. Mena-Osteritz, and P. Bauerle, New J. Chem. **23**, 241 (1999).
[66] G. Bidan, A. De Nicola, V. Enee, and S. Guillerez, Chem. Mater. Sci. **10**, 1052 (1998).
[67] W. J. Li, T. Maddux, and L. P. Yu, Macromolecules **29**, 7329 (1996).
[68] G. Barbarella, A. Bongini, and M. Zambianchi, Macromolecules **27**, 3039 (1994).
[69] U. Scherf, J. Mater. Chem. **9**, 1853 (1999).
[70] A. Köhler, J. Grüner, R. H. Friend, K. Müllen, and U. Scherf, Chem. Phys. Lett. **243**, 456 (1995).
[71] G. Weiser and S. Moller, Phys. Rev. B **6504**, 045203 (2002).
[72] D. Emin, Phys. Rev. B **33**, 3973 (1986).
[73] D. Emin and M. N. Bussac, Phys. Rev. B **49**, 14 290 (1994).
[74] D. Baeriswyl and K. Maki, Synth. Met. **28**, D507 (1989).
[75] H. A. Mizes and E. M. Conwell, Phys. Rev. Lett. **70**, 1505 (1993).